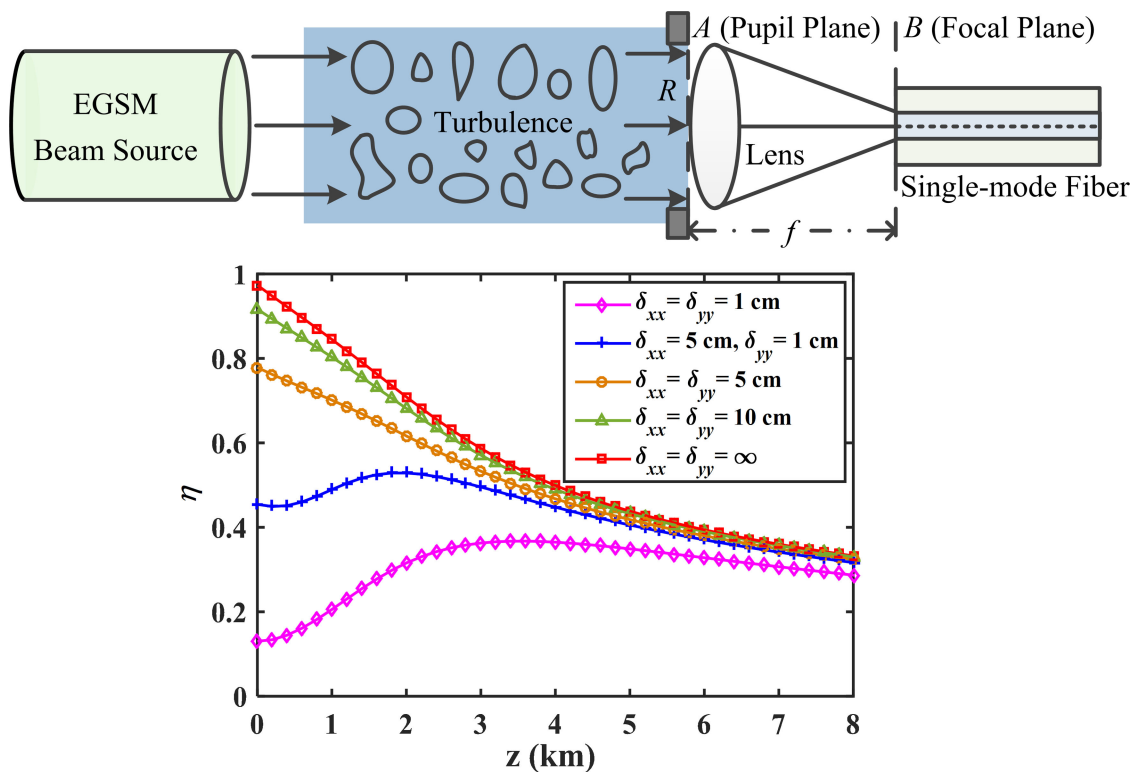


Free-Space to Fiber Coupling of Electromagnetic Gaussian Schell-Model Beams in Turbulent Marine Atmospheric Channel

Volume 10, Number 6, December 2018

Lin Yu
Yixin Zhang



Free-Space to Fiber Coupling of Electromagnetic Gaussian Schell-Model Beams in Turbulent Marine Atmospheric Channel

Lin Yu  1,2 and Yixin Zhang  1,2

¹School of Science, Jiangnan University, Wuxi 214122, China

²Jiangsu Provincial Research Center of Light Industrial Optoelectronic Engineering and Technology, Wuxi 214122, China

DOI: 10.1109/JPHOT.2018.2874270

1943-0655 © 2018 IEEE. Translations and content mining are permitted for academic research only.
Personal use is also permitted, but republication/redistribution requires IEEE permission.
See http://www.ieee.org/publications_standards/publications/rights/index.html for more information.

Manuscript received August 1, 2018; revised September 23, 2018; accepted October 2, 2018. Date of publication October 9, 2018; date of current version October 18, 2018. This work was supported by the Fundamental Research Funds for the Central Universities of China under Grants JUSRP11721 and JUSRP51721B. Corresponding author: Y. Zhang (e-mail: zyx@jiangnan.edu.cn.)

Abstract: We present a method to analyze the fiber coupling efficiency η of electromagnetic Gaussian Schell-model (EGSM) beams propagating through marine atmospheric turbulence. The expression for η is derived from the relation of field distributions between EGSM beam and fiber mode. The influence factors of η are discussed, including the properties of EGSM beam, focusing lens, and turbulence. We find that η declines as the turbulence enhances. A large-aperture lens and an EGSM beam with high coherence, long wavelength, and optimum beam width are able to achieve a higher η in turbulent links. Beam polarization also takes effect on η but the effect is complex. Our investigation has applications in the fiber coupling of vectorial beams in communication systems.

Index Terms: Electromagnetic Gaussian Schell-model (EGSM) beams, fiber coupling, atmospheric turbulence, free-space optical communication.

1. Introduction

Coupling free-space beams into single-mode fiber has widespread applications in optical communication links, such as space-to-ground or the last mile links [1], [2]. Due to the ability to integrate with erbium-doped fiber amplifier, fiber-optic detectors are used as receivers to improve signal quality for further demodulation or transmission. This leads to demands for optimizing fiber coupling of beams and attracts much research interest. The way to improve coupling performances, especially the coupling efficiency, has become a focus [3]–[7].

When beams are coupled into fiber in practical free-space communication link, the effects of atmospheric turbulence are inevitable [3]. Dikmelik *et al.* established a theoretical model to analyze the fiber coupling efficiency of a plane wave, and found that the efficiency was degraded by turbulence [4]. Liu *et al.* discussed the wave-front aberrations of a plane wave caused by terrestrial atmospheric turbulence, including their impacts on fiber coupling efficiency and correction methods [5]. Tan *et al.* considered the influence of source coherence, and extended their investigation to partially coherent Gaussian Schell-model beams [6]. Wright *et al.* gave a demonstration of fiber

coupling of Gaussian laser beam in a low Earth orbiting space to ground channel by use of an adaptive optical correction system [7].

Although fiber coupling of scalar beams mentioned above has been studied widely, the case of vectorial electromagnetic beams is still to be explored. Electromagnetic beams contain both coherence and polarization properties, which offer more adjustable parameters for applications [8]–[10]. Taking the electromagnetic Gaussian Schell-model (EGSM) beam as example, Salem *et al.* derived a theoretical formula to predict its coupling efficiency into fiber [11]. Later, an experimental coupling demonstration was conducted by Zhao *et al.* [12]. In these early explorations, the receiving fiber was located at or near the source plane, so the process of beam propagation before coupling was ignored. However, when considering the long-distance propagation from beam source to receiver, especially through turbulent atmosphere in communication links, the fiber coupling properties of EGSM beam haven't been reported.

In this paper, we investigate the single-mode fiber coupling of EGSM beam in marine atmospheric turbulence. Based on the cross spectral density matrix for unified description of coherence and polarization, a theoretical model is built for numerical calculation of fiber coupling efficiency. With full consideration of beam, turbulence and focusing lens, the influence factors of coupling efficiency are discussed in details. The results are helpful in designing the optimum fiber coupling system for EGSM beams in optical communication applications.

2. Fiber Coupling Efficiency in Turbulence

The effects of atmospheric turbulence on fiber coupling of free-space beams are mainly determined by turbulence intensity S . S reflects the level of atmospheric refractive-index fluctuation, which causes the distortion of free-space beams. As for marine atmospheric turbulence, the power spectrum density Φ of refractive-index fluctuation is given by [13]

$$\Phi(\kappa) = 0.033C_n^2 \left[1 - 0.061\frac{\kappa}{\kappa_H} + 2.836\left(\frac{\kappa}{\kappa_H}\right)^{7/6} \right] \frac{\exp(-\kappa^2/\kappa_H^2)}{(\kappa^2 + \kappa_0^2)^{11/6}}, \quad (1)$$

where κ is the spatial frequency, C_n^2 is the refractive-index structure constant, l_0 and L_0 are the inner scale and outer scale of turbulence respectively, $\kappa_H = 3.41/l_0$ and $\kappa_0 = 2\pi/L_0$.

With the help of the formula [14]

$$\int_0^\infty \kappa^{2a} \frac{\exp(-\kappa^2/\kappa_m^2)}{(\kappa^2 + \kappa_n^2)^b} d\kappa = \frac{1}{2} \kappa_n^{2a+1-2b} \Gamma\left(a + \frac{1}{2}\right) U\left(a + \frac{1}{2}; a - \frac{1}{3}; \frac{\kappa_n^2}{\kappa_m^2}\right) \quad [a > -0.5], \quad (2)$$

the analytic expression of S is obtained through the integral of $\Phi(\kappa)$ as follows

$$\begin{aligned} S &= \int_0^\infty \kappa^3 \Phi(\kappa) d\kappa \\ &= 0.0165 C_n^2 \kappa_0^{1/3} \left[U\left(2; \frac{7}{6}; \frac{\kappa_0^2}{\kappa_H^2}\right) - 0.081 \frac{\kappa_0}{\kappa_H} U\left(\frac{5}{2}; \frac{5}{3}; \frac{\kappa_0^2}{\kappa_H^2}\right) + 4.004 \left(\frac{\kappa_0}{\kappa_H}\right)^{7/6} U\left(\frac{31}{12}; \frac{7}{4}; \frac{\kappa_0^2}{\kappa_H^2}\right) \right], \end{aligned} \quad (3)$$

where $\Gamma(\cdot)$ is the gamma function, $U(\cdot)$ is the confluent hypergeometric function of the second kind. In this way, all the turbulence parameters are included in one expression of S , which facilitates the later analysis of turbulence effects.

To investigate the effects of beam properties, the cross spectral density (CSD) matrix is vital according to the unified theory of coherence and polarization for vectorial beams [15]. As for an EGSM beam, the components in CSD matrix at the source plane are given by [8]

$$W_{0uv}(r_{01}, r_{02}) = A_u A_v B_{uv} \exp\left[-\left(\frac{r_{01}^2}{4\sigma_u^2} + \frac{r_{02}^2}{4\sigma_v^2}\right)\right] \exp\left[-\frac{(r_{01} - r_{02})^2}{2\delta_{uv}^2}\right], \quad (4)$$

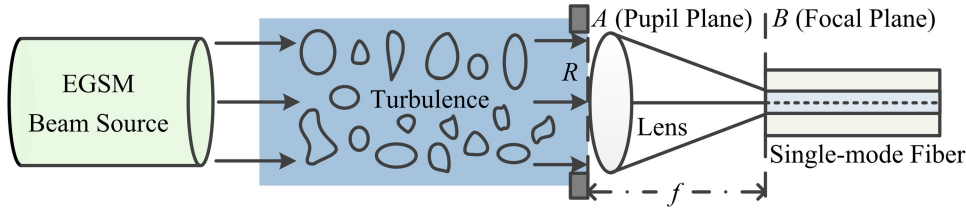


Fig. 1. Schematic of fiber coupling of EGSM beam in turbulent channel.

where \mathbf{r}_{01} and \mathbf{r}_{02} are position vectors. Both u and v take values of x or y (i.e., $u = x, y$ and $v = x, y$), which indicate the direction of beam electric field along x or y axis. $A_u(A_v)$ and $\sigma_u(\sigma_v)$ are the field amplitude and beam width respectively in $u(v)$ direction, B_{uv} and δ_{uv} are the correlation coefficient and transverse coherent width between field components in u and v directions respectively. In the case of $u = v$, $B_{uv} = 1$; otherwise $B_{uv} < 1$.

When an EGSM beam propagates a distance of z in the marine atmospheric turbulence, its CSD component W_{uv} at the receiver can be obtained by use of the extended Huygens-Fresnel principle. With consideration of the phase perturbation ψ caused by turbulence, W_{uv} is written as

$$W_{uv}(\mathbf{r}_1, \mathbf{r}_2) = \left(\frac{k}{2\pi z} \right)^2 \int \int \int \int W_{0uv}(\mathbf{r}_{01}, \mathbf{r}_{02}) \exp \left\{ -\frac{ik}{2z} [(\mathbf{r}_1 - \mathbf{r}_{01})^2 - (\mathbf{r}_2 - \mathbf{r}_{02})^2] \right\} \times \langle \exp [\psi(\mathbf{r}_1, \mathbf{r}_{01}, z) + \psi(\mathbf{r}_2, \mathbf{r}_{02}, z)] \rangle d^2 \mathbf{r}_{01} d^2 \mathbf{r}_{02}. \quad (5)$$

where k is the beam's wavenumber inversely related to wavelength λ ($k = 2\pi/\lambda$), $\langle \cdot \rangle$ is the symbol for ensemble average. According to the quadratic approximation for Rytov phase structure function, the term in $\langle \cdot \rangle$ has an expansion of [16]

$$\langle \exp [\psi^*(\mathbf{r}_1, \mathbf{r}_{01}, z) + \psi(\mathbf{r}_2, \mathbf{r}_{02}, z)] \rangle = \exp \left\{ -\frac{S}{3} \pi^2 k^2 z [(\mathbf{r}_{01} - \mathbf{r}_{02})^2 + (\mathbf{r}_{01} - \mathbf{r}_{02})(\mathbf{r}_1 - \mathbf{r}_2) + (\mathbf{r}_1 - \mathbf{r}_2)^2] \right\}. \quad (6)$$

Now by use of W_{uv} , the beam incident power P_0 at the receiver (i.e., fiber end face) can be obtained directly, while the power P coupled into fiber needs calculation of the field overlapping between incident beam and fiber mode. Considering the beam focusing device in practical coupling system, an equivalent focusing lens is used in modeling, with fiber end face located at lens focal plane B (see Fig. 1). Due to the Fourier-transforming property of lens, the field distributions (including incident beam field and fiber mode field) at lens pupil plane A and focal plane B are Fourier transform conjugate pairs. According to the Parseval-Plancherel theorem, it is equivalent in principle to analyze P_0 , P and then coupling efficiency at plane A and B . However, for reason of calculation convenience [4], here plane A is selected for analysis.

Therefore, the fiber coupling efficiency η of EGSM beam is defined at plane A as

$$\begin{aligned} \eta &= \frac{P}{P_0} = \frac{\iint_A \iint_A \text{Tr} [\mathbf{W}(\mathbf{r}_1, \mathbf{r}_2) \cdot \mathbf{F}_A^\dagger(\mathbf{r}_1, \mathbf{r}_2)] d^2 \mathbf{r}_1 d^2 \mathbf{r}_2}{\iint_A \text{Tr} [\mathbf{W}(\mathbf{r}, \mathbf{r})] d^2 \mathbf{r}}, \\ \mathbf{W}(\mathbf{r}_1, \mathbf{r}_2) &= \begin{pmatrix} W_{xx}(\mathbf{r}_1, \mathbf{r}_2) & W_{xy}(\mathbf{r}_1, \mathbf{r}_2) \\ W_{yx}(\mathbf{r}_1, \mathbf{r}_2) & W_{yy}(\mathbf{r}_1, \mathbf{r}_2) \end{pmatrix}, \\ \mathbf{F}_A(\mathbf{r}_1, \mathbf{r}_2) &= \begin{pmatrix} F_{xA}^*(\mathbf{r}_1) F_{xA}(\mathbf{r}_2) & 0 \\ 0 & F_{yA}^*(\mathbf{r}_1) F_{yA}(\mathbf{r}_2) \end{pmatrix}, \end{aligned} \quad (7)$$

where \mathbf{W} is the CSD matrix of EGSM beam, \mathbf{F}_A is the backpropagated fiber mode field matrix at plane A (i.e., the Fourier transform of fiber mode field at plane B), Tr and \dagger denote the trace and Hermitian adjoint of matrix respectively in math. Due to the orthogonality between fiber modes along

x and y direction, the anti-diagonal elements of \mathbf{F}_A are zero. So after a simple matrix operation, Eq. (7) is rewritten as

$$\eta = \frac{\sum P_{uu}}{\sum P_{0uu}} (u = x, y), \quad (8)$$

$$P_{0uu} = \iint_A W_{uu}(\mathbf{r}, \mathbf{r}) d^2\mathbf{r}, \quad (9)$$

$$P_{uu} = \iint_A \iint_A W_{uu}(\mathbf{r}_1, \mathbf{r}_2) F_{uA}(\mathbf{r}_1) F_{uA}^*(\mathbf{r}_2) d^2\mathbf{r}_1 d^2\mathbf{r}_2. \quad (10)$$

In terms of single-mode fibers, the backpropagated fiber mode field is expressed as [17]

$$F_{uA}(\mathbf{r}) = \frac{\sqrt{2\pi}w_u}{\lambda f} \exp \left[-\left(\frac{\pi w_u r}{\lambda f} \right)^2 \right], \quad (11)$$

where w_u is the mode field radius at fiber end face, f is the focal length of lens. From Eqs. (8)–(10), we find that only the diagonal elements of \mathbf{W} contribute to η . By substituting Eqs. (4) and (6) into Eq. (5) with some algebraic transformations and integral operations, the analytic expression of W_{uu} is given by [18]

$$W_{uu}(\mathbf{r}_1, \mathbf{r}_2) = \frac{A_u^2}{\Delta_{uu}} \exp \left[-\frac{(\mathbf{r}_1 + \mathbf{r}_2)^2}{8\Delta_{uu}\sigma_u^2} \right] \exp \left[\frac{ik(r_2^2 - r_1^2)}{2H_{uu}} \right] \exp \left[-\left(\frac{1}{8\Delta_{uu}\sigma_u^2} + M_{uu} \right) (\mathbf{r}_1 - \mathbf{r}_2)^2 \right], \quad (12)$$

where the introduced parameters Δ_{uu} , H_{uu} and M_{uu} are

$$\begin{aligned} \Delta_{uu} &= 1 + \frac{z^2}{k^2\sigma_u^2} \left(\frac{1}{4\sigma_u^2} + \frac{1}{\delta_{uu}^2} \right) + \frac{2\pi^2 z^3 S}{3\sigma_u^2}, \\ H_{uu} &= \frac{3z\Delta_{uu}\sigma_u^2}{3(\Delta_{uu} - 1)\sigma_u^2 + \pi^2 z^3 S}, \\ M_{uu} &= \frac{1}{2\Delta_{uu}\delta_{uu}^2} + \frac{S}{3} \pi^2 k^2 z (1 + \sigma_u^2) - \frac{\pi^4 k^2 z^4 S^2}{18\Delta_{uu}\sigma_u^2}. \end{aligned} \quad (13)$$

Based on the results of Eqs. (11) and (12), as well as the law of cosines as follows:

$$(\mathbf{r}_1 \pm \mathbf{r}_2)^2 = r_1^2 + r_2^2 \pm 2r_1 r_2 \cos(\varphi_1 - \varphi_2), \quad (14)$$

the integrals in Eqs. (9) and (10) are expanded as

$$P_{0uu} = \frac{A_u^2}{\Delta_{uu}} \int_0^{2\pi} \int_0^R \exp \left(-\frac{r^2}{2\Delta_{uu}\sigma_u^2} \right) r dr d\varphi, \quad (15)$$

$$\begin{aligned} P_{uu} &= \frac{2\pi w_u^2 A_u^2}{\lambda^2 f^2 \Delta_{uu}} \int_0^{2\pi} \int_0^{2\pi} \int_0^R \int_0^R \exp \left[-\left(\frac{1}{4\Delta_{uu}\sigma_u^2} + \frac{\pi^2 w_u^2}{\lambda^2 f^2} + M_{uu} \right) (r_2^2 + r_1^2) \right] \\ &\quad \times \exp \left[\frac{ik(r_2^2 - r_1^2)}{2H_{uu}} \right] \exp [2M_{uu}r_1 r_2 \cos(\varphi_1 - \varphi_2)] r_1 r_2 dr_1 dr_2 d\varphi_1 d\varphi_2. \end{aligned} \quad (16)$$

where R is the receiver aperture radius (i.e., lens radius) at plane A . Then performing the integrations in Eqs. (15) and (16) over φ , φ_1 or φ_2 , with the help of the property of Bessel function as follows:

$$\int_0^{2\pi} \exp [\varpi \cos(\varphi_1 - \varphi_2)] d\varphi_1 = 2\pi I_0(\varpi), \quad (17)$$

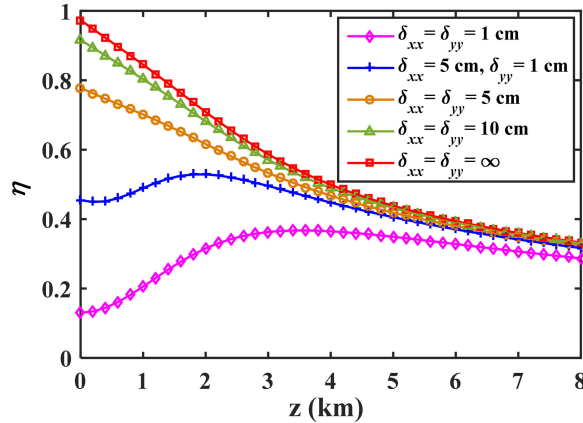


Fig. 2. Fiber coupling efficiency η in relation to the propagation distance z and source coherent widths δ_{xx}, δ_{yy} of EGSM beam.

the simplified expressions of P_{0uu} and P_{uu} are given by

$$P_{0uu} = 2\pi A_u^2 \sigma_u^2 \left[1 - \exp \left(-\frac{R^2}{2\Delta_{uu}\sigma_u^2} \right) \right], \quad (18)$$

$$\begin{aligned} P_{uu} = & \frac{8\pi^3 w_u^2 A_u^2}{\lambda^2 f^2 \Delta_{uu}} \int_0^R \int_0^R \exp \left[-\left(\frac{1}{4\Delta_{uu}\sigma_u^2} + \frac{\pi^2 w_u^2}{\lambda^2 f^2} + M_{uu} \right) (r_2^2 + r_1^2) \right] \\ & \times \exp \left[\frac{ik(r_2^2 - r_1^2)}{2H_{uu}} \right] I_0 (2M_{uu} r_1 r_2) r_1 r_2 dr_1 dr_2, \end{aligned} \quad (19)$$

where $I_0(\cdot)$ is the modified Bessel function of the first kind. Normalizing the integral variables by $\xi_1 = r_1/R$ and $\xi_2 = r_2/R$, Eq. (19) is rewritten as

$$\begin{aligned} P_{uu} = & \frac{8\pi^3 w_u^2 A_u^2 R^4}{\lambda^2 f^2 \Delta_{uu}} \int_0^1 \int_0^1 \exp \left[-\left(\frac{R^2}{4\Delta_{uu}\sigma_u^2} + \frac{\pi^2 w_u^2 R^2}{\lambda^2 f^2} + M_{uu} R^2 \right) (\xi_2^2 + \xi_1^2) \right] \\ & \times \exp \left[\frac{ikR^2 (\xi_2^2 - \xi_1^2)}{2H_{uu}} \right] I_0 (2M_{uu} R^2 \xi_1 \xi_2) \xi_1 \xi_2 d\xi_1 d\xi_2. \end{aligned} \quad (20)$$

By substituting Eqs. (3), (13), (18) and (20) into Eq. (8), numerical analysis on the fiber coupling efficiency of EGSM beam in marine atmospheric turbulence is accessible, from which some useful conclusions on beam optimization can be drawn.

3. Analysis of Coupling Efficiency for EGSM Beam

In this section, different conditions are simulated to investigate the coupling of EGSM beam into single-mode fiber in turbulent marine atmospheric link. The influence factors on coupling efficiency such as beam properties, turbulence level and lens size are discussed in details. Unless otherwise indicated in figures, the parameters used for simulations have typical values as follows [6], [8], [13]: $C_n^2 = 10^{-15} \text{ m}^{-2/3}$, $l_0 = 1 \text{ mm}$, $L_0 = 1 \text{ m}$, $z = 1 \text{ km}$, $R = 5 \text{ cm}$, $f = 35 \text{ cm}$, $\lambda = 1.55 \mu\text{m}$, $w_x = w_y = 5 \mu\text{m}$, $A_x = A_y = 1$, $\sigma_x = \sigma_y = 2 \text{ cm}$ and $\delta_{xx} = \delta_{yy} = 10 \text{ cm}$.

Considering the two significant properties (i.e., coherence and polarization) of EGSM beam, the relationships between coupling efficiency η and beam transverse coherent widths δ_{xx}, δ_{yy} are analyzed in Fig. 2 first. With the increase of either δ_{xx} or δ_{yy} , source coherence increases and a larger η is obtained. When δ_{xx} and δ_{yy} tend to infinity, the partially coherent beam source evolves into a fully coherent one, and η reaches the maximum. However, under different conditions of δ_{xx}

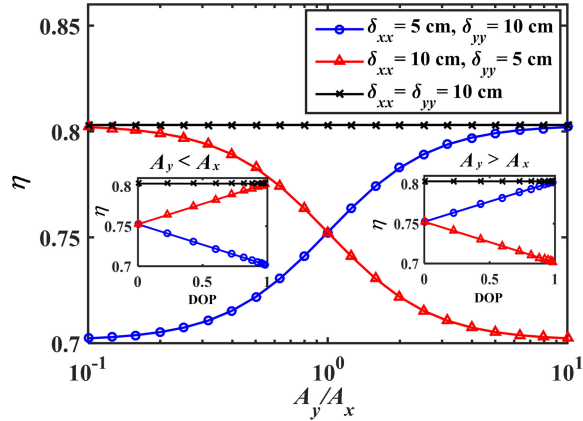


Fig. 3. Fiber coupling efficiency η in relation to the source polarization parameter A_y/A_x of EGSM beam.

and δ_{yy} , the variation curves of η with the propagation distance z are different before converging. This is attributed to the co-work of beam diffraction broadening and atmospheric turbulence. When a beam propagates in free space, diffraction broadening occurs. In the absence of turbulence, the increment of beam spatial coherence with diffraction broadening causes the rise of η [6]. But in practical atmospheric link, turbulence is inevitable, which reduces beam coherence and in turn η during propagation. So with the increase of z , η rises when beam broadening is dominant, but declines when turbulence is dominant. Considering that a beam with larger δ_{xx} and δ_{yy} always has a larger η , a high coherent EGSM beam or even a fully coherent electromagnetic Gaussian beam is preferred for fiber coupling in turbulent marine atmospheric link.

Figure 3 discusses the relationship between fiber coupling efficiency and source polarization of EGSM beam. In the case of $\sigma_x = \sigma_y$, the ratio of the field amplitude in y and x direction A_y/A_x is varied to change the source polarization. We find that the variation of η with A_y/A_x is complexly related to the source coherent widths δ_{xx} , δ_{yy} . If $\delta_{yy} > \delta_{xx}$ ($\delta_{yy} < \delta_{xx}$), η rises (declines) as A_y/A_x increases, but if $\delta_{yy} = \delta_{xx}$, the variation of A_y/A_x doesn't affect η . To describe beam polarization quantitatively, the degree of polarization (DOP) is used. As shown in Eq. (7), η is independent of the anti-diagonal elements of the CSD matrix W . If a beam without the anti-diagonal elements of W (i.e., the corresponding coefficients $B_{xy} = B_{yx} = 0$) is used, DOP is only the function of A_y/A_x as follows [8]

$$\text{DOP} = \frac{\sqrt{(A_x^2 - A_y^2)^2 + 4A_x^2 A_y^2 |B_{xy}|^2}}{A_x^2 + A_y^2} = \frac{|1 - A_y^2/A_x^2|}{1 + A_y^2/A_x^2}. \quad (21)$$

When DOP increases from 0 to 1, the unpolarized beam evolves to be fully polarized. Considering that DOP is not monotonous with A_y/A_x , the insets in Fig. 3 give the variations of η with DOP for the case of $A_y < A_x$ and $A_y > A_x$. The insets also reveal that beam polarization affects η complexly and the effect is related to beam coherence.

To investigate the influence of beam width on η , several values of σ_x and σ_y no more than lens radius are selected. As for a focusing lens with the fixed focal length, the backpropagated fiber mode field at the lens pupil plane A is constant, so the beam size in best match with fiber mode results in the highest η , and there exists the optimum beam width for coupling, just as shown in Fig. 4. Under different values of $\sigma_x(\sigma_y)$, the optimum $\sigma_y(\sigma_x)$ and the maximum available η are different. This is because in the case of asymmetric beam with $\sigma_x \neq \sigma_y$, the incident power coupled into fiber in one direction is different from the other. So if $\sigma_x(\sigma_y)$ is fixed, the optimum $\sigma_y(\sigma_x)$ is related to $\sigma_x(\sigma_y)$ considering their weights on power coupling.

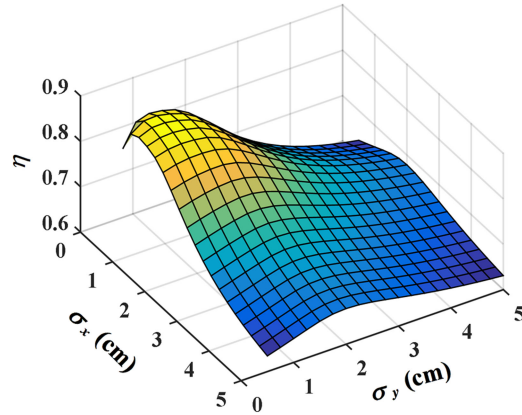


Fig. 4. Fiber coupling efficiency η in relation to the waist widths σ_x , σ_y of EGSM beam.

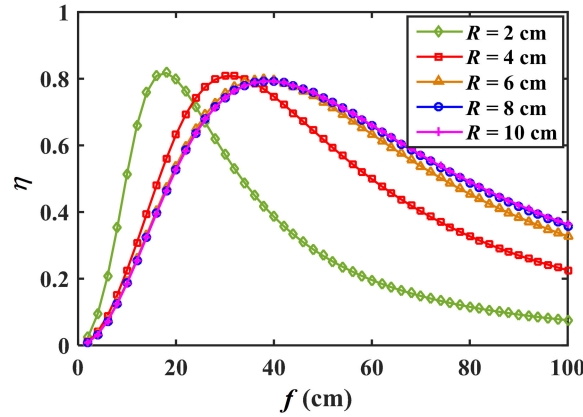


Fig. 5. Fiber coupling efficiency η in relation to the radius R and focal length f of the focusing lens.

Since the lens radius R limits the incident EGSM beam size and the lens focal length f affects the backpropagated fiber mode size, Fig. 5 investigates η under different R and f . When R is large enough, the incident beam is fully received for coupling. So the variation of η with f is independent of R , and only determined by the field matching between incident beam and fiber mode at the lens pupil plane. However, if the incident beam is truncated by R , the optimum f increases as R increases, to enlarge the overlapping region of field distributions between EGSM beam and fiber mode. Comparing the $\eta - f$ curves in Fig. 5, the curves corresponding to larger R are smoother, revealing that their η have better tolerance to the deviation of f from the optimum value. So the selection of a large-aperture lens is important for resisting interferences in practical optical system.

The effects of marine atmospheric turbulence on the fiber coupling efficiency of EGSM beam are determined by turbulence intensity S . Since S combines the contributions of the refractive-index structure constant C_n^2 , turbulence inner scale factor l_0 and outer scale factor L_0 , we first discuss the variation of η with C_n^2 in Fig. 6, then analyze the impacts of l_0 and L_0 in Fig. 7.

As C_n^2 increases, turbulence strengthens and causes a larger beam distortion [16]. The worse matching between the distorted EGSM beam and fiber mode inevitably degrades η , just as shown in Fig. 6. To achieve a higher η in turbulent channel, several common wavelengths in fiber communication window are compared. We find that EGSM beam with longer wavelength is more suitable for fiber coupling.

In terms of l_0 and L_0 , Fig. 7 shows that η rises with the increment of l_0 and the decrement of L_0 . This is because as l_0 increases or L_0 decreases, there are fewer turbulence eddies in the inertial

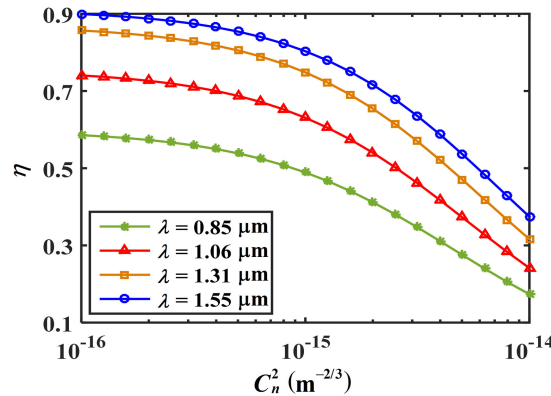


Fig. 6. Fiber coupling efficiency η in relation to turbulence refractive-index structure constant C_n^2 and EGSM beam wavelength λ .

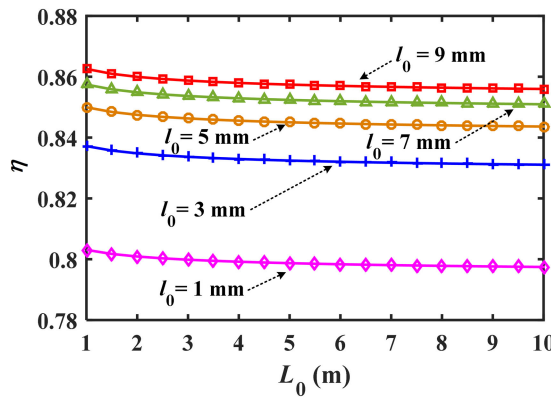


Fig. 7. Fiber coupling efficiency η in relation to the inner scale l_0 and outer scale L_0 of marine atmospheric turbulence.

range of turbulence, which weakens turbulence intensity consequently [16]. On the other hand, the variation of η with L_0 is so slight that can be ignored. The effect of l_0 on η is also weaker than that of C_n^2 . All these reveal that as for the marine atmospheric turbulence, the refractive-index structure constant is more important than scale factors in determining the turbulence intensity, as well as the coupling efficiency of EGSM beam into fiber.

4. Conclusions

Aiming at the coupling of EGSM beam into single-mode fiber, we establish a theoretical model to analyze the coupling efficiency η in the presence of marine atmospheric turbulence. By use of the cross spectral density matrix of EGSM beam and fiber mode field matrix, the numerical expression of η is derived and several simulations are conducted. The results reveal that η declines if turbulence strengthens (i.e., the increment of C_n^2 , L_0 or the decrement of l_0). A large-aperture lens with moderate focal length, and a long-wavelength beam with moderate beam width, are beneficial to improving η .

In terms of the two significant properties (coherence and polarization) of EGSM beam, the effect of polarization on η is complex and dependent on coherence. Since η rises with the increment of source coherence, a fully coherent beam can be regarded as an ideal choice if a high η is needed to reduce the power budget of communication link. However, in some applications which are sensitive to the received intensity fluctuations, a partially coherent beam is better because it has

less scintillation through atmospheric turbulence than the coherent one [19]. So in these situations, the selection of a partially coherent EGSM beam with relatively higher coherence is preferred to achieve a balance between η and scintillation. The research is hoped to give useful references for the design of beam coupling systems in free-space to fiber communications.

References

- [1] B. S. Robinson, C. M. Schieler, and D. M. Boroson, "Large-volume data delivery from low-earth orbit to ground using efficient single-mode optical receivers," *Proc. SPIE*, vol. 9739, Mar. 2016, Art. no. 97390A.
- [2] M. A. Esmail, A. Ragheb, H. Fathallah, and M. S. Alouini, "Investigation and demonstration of high speed full-optical hybrid FSO/fiber communication system under light sand storm condition," *IEEE Photon. J.*, vol. 9, no. 1, Feb. 2017, Art. no. 7900612.
- [3] L. Canuet *et al.*, "Statistical properties of single-mode fiber coupling of satellite-to-ground laser links partially corrected by adaptive optics," *J. Opt. Soc. Am. A*, vol. 35, no. 1, pp. 148–162, Jan. 2018.
- [4] Y. Dikmelik and F. M. Davidson, "Fiber-coupling efficiency for free-space optical communication through atmospheric turbulence," *Appl. Opt.*, vol. 44, no. 23, pp. 4946–4952, Aug. 2005.
- [5] W. Liu, W. Shi, K. Yao, J. Cao, P. Wu, and X. Chi, "Fiber coupling efficiency analysis of free space optical communication systems with holographic modal wave-front sensor," *Opt. Laser Technol.*, vol. 60, pp. 116–123, Aug. 2014.
- [6] L. Tan, M. Li, Q. Yang, and J. Ma, "Fiber-coupling efficiency of Gaussian Schell model for optical communication through atmospheric turbulence," *Appl. Opt.*, vol. 54, no. 9, pp. 2318–2325, Mar. 2015.
- [7] M. W. Wright, J. F. Morris, J. M. Kovalik, K. S. Andrews, M. J. Abrahamson, and A. Biswas, "Adaptive optics correction into single mode fiber for a low Earth orbiting space to ground optical communication link using the OPALS downlink," *Opt. Exp.*, vol. 23, no. 26, pp. 33705–33712, Dec. 2015.
- [8] O. Korotkova, M. Salem, and E. Wolf, "The far-zone behavior of the degree of polarization of electromagnetic beams propagating through atmospheric turbulence," *Opt. Commun.*, vol. 233, no. 4–6, pp. 225–230, Apr. 2004.
- [9] X. Chen, C. Chang, Z. Chen, Z. Lin, and J. Pu, "Generation of stochastic electromagnetic beams with complete controllable coherence," *Opt. Exp.*, vol. 24, no. 19, pp. 21587–21596, Sep. 2016.
- [10] M. Guo and D. Zhao, "Polarization properties of stochastic electromagnetic beams modulated by a wavefront-folding interferometer," *Opt. Exp.*, vol. 26, no. 7, pp. 8581–8593, Apr. 2018.
- [11] M. Salem and G. P. Agrawal, "Effects of coherence and polarization on the coupling of stochastic electromagnetic beams into optical fibers: Errata," *J. Opt. Soc. Am. A*, vol. 28, no. 3, p. 307, Mar. 2011.
- [12] C. Zhao, Y. Dong, G. Wu, F. Wang, Y. Cai, and O. Korotkova, "Experimental demonstration of coupling of an electromagnetic Gaussian Schell-model beam into a single-mode optical fiber," *Appl. Phys. B*, vol. 108, no. 4, pp. 891–895, Sep. 2012.
- [13] K. Y. Grayshan, F. S. Veltelino, and C. Y. Young, "A marine atmospheric spectrum for laser propagation," *Wave Random Complex*, vol. 18, no. 1, pp. 173–184, Jan. 2008.
- [14] I. S. Gradshteyn and I. M. Ryzhik, *Table of Integrals, Series, and Products*, Burlington, MA, USA: Academic, 2007.
- [15] E. Wolf, "Unified theory of coherence and polarization of random electromagnetic beams," *Phys. Lett. A*, vol. 312, no. 5–6, pp. 263–267, Jun. 2003.
- [16] L. C. Andrews and R. L. Phillips, *Laser Beam Propagation Through Random Media*, Bellingham, WA, USA: SPIE, 2005.
- [17] J. A. Buck, *Fundamentals of Optical Fibers*, Hoboken, NJ, USA: Wiley, 2004.
- [18] W. Lu, L. Liu, J. Sun, Q. Yang, and Y. Zhu, "Change in degree of coherence of partially coherent electromagnetic beams propagating through atmospheric turbulence," *Opt. Commun.*, vol. 271, no. 1, pp. 1–8, Mar. 2007.
- [19] G. Gbur, "Partially coherent beam propagation in atmospheric turbulence," *J. Opt. Soc. Am. A*, vol. 31, no. 9, pp. 2038–2045, Sep. 2014.